Cell and Tissue Research (2019) 376:295–308
https://doi.org/10.1007/s00441-019-02990-3

REGULAR ARTICLE

Oxidative stress modulates the expression of apoptosis-associated microRNAs in bovine granulosa cells in vitro

Md Mahmodul Hasan Sohel[1,2] · Bilal Akyuz[3] · Yusuf Konca[2] · Korhan Arslan[3] · Serpil Sariozkan[4] · Mehmet Ulas Cinar[2]

Received: 7 March 2018 / Accepted: 2 January 2019 / Published online: 21 January 2019

Abstract

Despite its essential role in ovulation, oxidative stress (OS) has been found to be cytotoxic to cells, while microRNAs (miRNAs) are known as a major regulator of genes involved in cellular defense against cytotoxicity. However, a functional link between OS and miRNA expression changes in granulosa cells (GCs) remains to be investigated. Here, we investigate the OS modulation of apoptosis-associated miRNAs and their biological relevance in bovine GCs. Following the evaluation of cell viability, accumulation of reactive oxygen species (ROS), cytotoxicity and mitochondrial activity, we used a ready-to-use miRNA PCR array to identify differentially regulated miRNAs. The results showed that exposure to 150 μM H_2O_2 for 4 h creates remarkable signs of OS in GCs characterized by more than 50% loss of cell viability, higher nuclear factor erythroid 2–related factor 2 (NRF2) nuclear translocation, significantly ($p < 0.05$) higher abundance of antioxidant genes, significantly ($p < 0.001$) higher accumulation of ROS, lower mitochondrial activity and a higher ($p < 0.001$) number of apoptotic nuclei compared to that of the control group. miRNA expression analysis revealed that a total of 69 miRNAs were differentially regulated in which 47 and 22 miRNAs were up- and downregulated, respectively, in stressed GCs. By applying the 2-fold and $p < 0.05$ criteria, we found 16 miRNAs were upregulated and 10 miRNAs were downregulated. Target prediction revealed that up- and downregulated miRNAs potentially targeted a total of 6210 and 3575 genes, respectively. Pathway analysis showed that upregulated miRNAs are targeting the genes involved mostly in cell survival, intracellular communication and homeostasis, cellular migration and growth control and disease pathways. Our results showed that OS modulates the expression of apoptosis-associated miRNAs that might have effects on cellular or molecular damages.

Keywords microRNA · Oxidative stress · Granulosa cells · Apoptosis · Signaling pathways

Introduction

Folliculogenesis is a dynamic and complex process and believed to be modulated by an orchestrated action of different hormones, local ovarian factors and spatiotemporal expression of several genes and miRNAs (Donadeu et al. 2012; Sohel and Cinar 2015). At the end of follicular development, granulosa cells (GCs) started transforming into granulosa-lutein cells by a preovulatory pituitary luteinizing hormone (LH) surge (Duffy and Stouffer 2003). This transformation is very important for a successful ovulation and subsequent formation of corpus luteum to maintain pregnancy. After the LH surge, at the time of ovulation, inflammatory cells (neutrophils and macrophages) are massively recruited at the site of follicular rupture and produce excessive reactive oxygen species (ROS) and their depletion impairs ovulation (Shkolnik et al. 2011). Acute inflammation caused by excessive ROS enhances follicular rupture and facilitates the release of oocyte cumulus complex. Therefore, it is highly likely that GCs are exposed to an excessive level of ROS and face OS during ovulation. On the other hand, overproduction of ROS is a major cause of GC apoptosis in follicular atresia (Agarwal et al. 2012). In addition, it has been reported that ROS may

Electronic supplementary material The online version of this article (https://doi.org/10.1007/s00441-019-02990-3) contains supplementary material, which is available to authorized users.

✉ Md Mahmodul Hasan Sohel
sohel@erciyes.edu.tr

[1] Genome and Stem Cell Centre, Erciyes University, 38039 Kayseri, Turkey

[2] Department of Animal Science, Faculty of Agriculture, Erciyes University, 38039 Kayseri, Turkey

[3] Department of Genetics, Faculty of Veterinary Science, Erciyes University, 38039 Kayseri, Turkey

[4] Department of Fertility and Artificial Insemination, Faculty of Veterinary Science, Erciyes University, 38039 Kayseri, Turkey

alter the GC hormone production, particularly estradiol 2 (Appasamy et al. 2008), which is further impacted by hormonal stimulation due to the excessive production of ROS (Ávila et al. 2016). An increased level of ROS negatively affects the reproductive potential and is associated with poor oocyte quality, suboptimal embryonic development and decreased female fertility (Al-Gubory et al. 2010; Ávila et al. 2016). It appears that there is an existence of a complex relationship between female reproduction and OS.

OS is characterized by an imbalance between the production of ROS and ROS scavenging ability of antioxidants. Cellular ROS is a byproduct of aerobic metabolism, generated and released from the mitochondria through leakage of an electron transport chain during oxidative phosphorylation and the tricarboxylic acid cycle (Ray et al. 2012). ROS can also be generated from the cellular response to exogenous toxic material such as xenobiotics, cytokines and bacterial invasion (Ray et al. 2012). Depending on the level of abundance, ROS can activate different pathways. For instance, a lower level of ROS can activate survival pathways, whereas a higher level can initiate pathways related to cellular apoptosis in bovine GCs (Sohel et al. 2017). In addition to the other factors, the role of miRNAs in activating survival or apoptotic pathways cannot be overruled.

miRNAs are endogenously initiated non-coding RNA species of 18–22 nucleotides long and are considered one of the major post-transcriptional regulators of gene expression (Hossain et al. 2012). Since their discovery, miRNAs have been found to be involved in various biological processes including differentiation, proliferation, development and apoptosis (Sohel 2016). In addition, aberrant miRNA expression has been shown to be associated with diseases like diabetics (Simpson et al. 2016), cardiovascular disease (Romaine et al. 2015), cancer (Peng and Croce 2016) and reproductive dysfunctions (Tesfaye et al. 2017). Furthermore, conditional knockout of Dicer, a miRNA processing gene, results in impaired folliculogenesis, premature ovarian failure and female infertility (Nagaraja et al. 2008; Yuan et al. 2014), development of sterile Müllerian duct and uterus (Gonzalez and Behringer 2009; Hawkins et al. 2012) and development of reproductive (Hong et al. 2008) and urogenital tract (Pastorelli et al. 2009) in mouse model indicating the importance of miRNA in reproduction. We previously reported that an excessive level of ROS produced by H_2O_2 was extremely cytotoxic to GCs in cell culture and caused a higher cell death (Sohel et al. 2016). In addition, the role of a specific miRNA in GC apoptosis under OS has been recently demonstrated (Xu et al. 2017). However, how OS modulates the expression of an array of apoptosis-associated miRNAs in GCs is poorly understood. Therefore, this study aims to elucidate the role of H_2O_2-induced OS in modulating the abundance of apoptosis-associated miRNAs and to understand their potential biological relevance in bovine GCs exposed to OS.

Materials and methods

Ovary and GC collection

Bovine GCs were collected and cultured according to a previous protocol (Sohel et al. 2013). Briefly, ovaries were collected from a local abattoir and kept at 0.9% saline solution in a thermoflask. In the laboratory, following two washes with a prewarm saline solution and 70% ethanol, the follicular materials (follicular fluid containing GCs) were collected from preovulatory follicles (13–18 mm in diameter) by a 5-mL syringe with an 18-gauge needle and placed in a 50-mL sterile falcon tube containing 10-mL TCM media. GCs from preovulatory follicles are closer to the biological states (ovulation) than growing follicles (4–8 mm in diameter). After collection of all samples, tubes were left for 15 min at 37 °C to allow the oocyte cumulus complex and cellular debris to be settled at the bottom. The upper liquid containing GCs was transferred to a new 15-mL tube followed by a centrifugation at 500×*g* for 5 min to obtain the GCs.

Culture and treatment of GCs

After washing with calcium-magnesium-free PBS (CMF), GC pellets were resuspended in 1 mL of red blood cell lysis buffer (8.26 mg of NH_4Cl/mL in 10 mM Tris-HCl/L buffer) for 1 min. GCs were washed twice with culture media and approximately 10,000, 2×10^5 and 1.5×10^6 viable cells were seeded in 96-well, 24-well and 6-well culture plates, respectively and cultured in DMEM/F-12 medium containing 10% FBS, penicillin (100 U/mL) and streptomycin (100 μg/mL) under optimum culture conditions (37 °C, humidified and 5% CO_2) until 40–50% confluence. These conditions are optimum to maintain GCs in the non-luteinized state for 3–4 days. To induce OS, primary cultures of GCs were exposed to 150 μM H_2O_2 (Sigma-Aldrich; Darmstadt, Germany) in culture media for 4 h under optimum culture conditions. This concentration was selected based on our experiences in the lab (Sohel et al. 2016). Following the treatments, cells were either investigated for different morphological characteristics or disassociated from culture plate using trypsin-EDTA, collected and stored at − 80 °C for further genetic analysis. The purity of isolated GC was determined by the presence of FSHR (GC-specific marker) and the absence of CYP17A1 (theca cell–specific marker) and the results are presented in the Electronic Supplementary Material Fig. S1. The sequence of the primers is listed in the Electronic Supplementary Material Table S1. The results showed that GC-specific marker gene FSHR was detected at a higher level as indicated by a strong band, while no expression was detected for the CYP17A1 gene in GCs. This result confirms the isolation procedure of GCs was completely free of contamination from theca cells.

Cell morphology and viability

Cells were routinely checked for cell morphology and confluence throughout the experiment in a Nikon Eclipse TS100 (Nikon, Tokyo, Japan) inverted microscope. The viability of cells was determined as previously described (Sohel et al. 2017). Briefly, both the floating and adherent cells were collected after the treatment period and diluted in 1 mL medium by gentle pipetting. Following that, 100 μL of cell suspension and 100 μL of 0.4% trypan blue dye were mixed gently and incubated for 1–2 min at room temperature. Ten microliters of cell mixture/trypan blue was applied to the hemocytometer and placed under a microscope for counting live and dead cells. Cell viability was calculated as follows: percentage of cell viability = (number of unstained cells/number of total cells) × 100.

Cell survival assay

Damaging effects of H_2O_2 on GCs was determined using the Cell Proliferation Reagent WST-1 (Roche Diagnostics GmbH, Mannheim, Germany) kit as it can be used as a substitute of MTT assay (Ngamwongsatit et al. 2008). Briefly, 10,000 viable GCs were plated in each well of 96-well microplate (Clear, Flat Bottom TC-Treated, Corning Incorporated) containing 100 μL/well culture media and continue culture up to 50% confluence in a humidified atmosphere (37 °C and 5% CO_2). Cells were treated according to the experimental plan. Following the culture period, 10 μL WST-1 reagent was added to each well of the microplate and incubated for 5 h at 37 °C under standard culture condition. After that, the microplate was shaken for 1 min and absorbance was measured using a microplate (ELISA) reader (Glomax Multi Detection System, Promega BioSystems Sunnyvale, CA, USA) with a wavelength of 460 nm. The GC survival was expressed using optical density value.

Detection of nuclear translocation of NRF2 using immunocytochemistry

Immunocytochemistry was performed in order to detect and localize NRF2 proteins in control and treated cells according to the previous protocol (Sohel et al. 2017). Briefly, 2×10^5 viable GCs were grown in each well of a 24-well culture plate. After the treatment period, GCs were washed with warm DPBS and fixed overnight in 4% paraformaldehyde at 4 °C. GCs were then washed three times with DPBS, permeabilized using 0.2% TritonX-100 (Sigma-Aldrich) in PBS at room temperature for 1 h and washed with DPBS three times, 5 min each. After blocking with 3% normal donkey serum in DPBS for 1 h at room temperature, cells were incubated overnight at 4 °C with a primary antibody specific to NRF2 (SC-722, Santa Cruz Biotechnology, Dallas, Texas; 1:100 dilution). In the next day, cells were washed twice with 0.05% Tween 20 (P9416, Sigma) in DPBS and incubated further with donkey anti-rabbit secondary antibody (SC-2090, FITC conjugated, Santa Cruz Biotechnology, Dallas, Texas; 1:200 dilution) for 1 h at 37 °C in the dark. Following two additional washes, cells were incubated for 5 min in the dark with 5 ng/mL 4′,6′-diamidino-2-phenylindole (DAPI; Vector Laboratories) in DPBS to stain the nucleus and fluorescence microscopy was performed with a Nikon Eclipse T*i*-S microscope (Nikon Instruments Inc., Tokyo, Japan; 20X magnification) using green and blue fluorescence filters and images were captured by NIS Elements software.

Intracellular ROS accumulation

ROS formation in GCs was evaluated using 6-carboxy-2′,7′-dichlorodihydrofluorescin diacetate (H_2DCFDA; Molecular Probes, Eugene, OR), a fluorescent dye that is sensitive to the formation of diverse types of ROS, according to the manufacturer's protocol. Briefly, following the treatment, 400 μL of 15 μM H_2DCFDA was added to each well of a 24-well plate and incubated for 20 min in the dark at 37 °C under standard culture condition. GCs were washed twice with DPBS and images were taken immediately with a Nikon Eclipse T*i*-S microscope (Nikon Instruments Inc., Tokyo, Japan) using a green fluorescence filter and images were acquired by NIS Elements software. The quantitative analysis of fluorescence data was analyzed by histogram analysis of fluorescence intensity across the image using ImageJ software (National Institutes of Health, Bethesda, MD, USA).

Mitochondrial activity

The activity of mitochondria ($n = 3$) was examined using MitoTracker1 Red CMXRos (M7512; Life Technologies, Oregon, USA), which is well retained after aldehyde fixation using the manufacturer's protocol. Briefly, GCs from different treatment groups were washed twice with DPBS and then 100 nM Mito Tracker red dye was added and incubated for 45 min. GCs were washed twice with DPBS and fixed overnight with 4% formaldehyde. On the next day, fixed cells were mounted with a mounting medium containing DAPI (H-1200, Vector Laboratories, Inc., CA, USA). Images were captured immediately using a fluorescence microscope (Nikon Eclipse T*i*-S microscope, Nikon Instruments Inc., Tokyo, Japan). The mean fluorescence intensity of five non-overlapping fields in each well was measured using ImageJ software.

Detection of apoptosis TUNEL assay

Apoptosis in GCs ($n = 3$) was analyzed by Terminal deoxynucleotidyl transferase (TdT) dUTP Nick-End

Labeling (TUNEL) assay using a Click-iT® Plus TUNEL Assay kit (Life Technologies, Inc., Carlsbad, CA, USA) according to the protocol described elsewhere (Sohel et al. 2017). Briefly, after the treatment period, 50 μL of TdT reaction mixture was added to each well of 96-well plates, incubated for 1 h at 37 °C and Alexa Fluor® 594 dye (red fluorescence) was added and incubated for 30 min. After that, cells were stained with 5 ng/mL DAPI (ThermoFisher Scientific) in PBS for 5 min and observed under a fluorescence microscope (Nikon Eclipse Ti-S microscope, Nikon Instruments Inc., Tokyo, Japan; 20X magnification) using red and blue fluorescence filters. TUNEL-positive and TUNEL-negative nuclei were counted from five non-overlapping fields per replicate and converted to percentages by comparing the total number of nuclei with TUNEL-positive nuclei.

Extraction of total RNA and cDNA synthesis

Total RNA was extracted from GCs using the miRNeasy mini kit (Qiagen, Hilden, Germany) according to the manufacturer's instruction. RNase-Free DNase set (Cat no. 79254, Qiagen, Hilden, Germany) was used during total RNA isolation in order to remove any additional DNA contamination. Concentration and total RNA purity were investigated by a BioSpec-nano spectrophotometer (Shimadzu Biotech, Japan). For miRNA PCR array, cDNA was synthesized using the miScript® II RT Kit (Cat. No. 218191, Qiagen, Hilden, Germany) according to the manufacturers' instruction. The cDNA synthesis reaction consists of 5× HiSpec Buffer (4 μL), miScript Reverse Transcriptase Mix (2 μL), 10× miScript Nucleics Mix (2 μL), water (variable) and template RNA (400 ng). First, the cDNA synthesis reaction was incubated at 37 °C for 60 min followed by 95 °C for 5-min incubation. The resulting cDNA was diluted according to the manufacturer's instructions for further use in miRNA PCR Array. For mRNA expression analysis, total RNA was reverse transcribed to cDNA using the Maxima H Minus First Strand cDNA Synthesis Kit (Thermo Scientific, Massachusetts, USA) according to the previous protocol (Sohel et al. 2017).

Real-time quantitative PCR for candidate genes

Roche Light cycler 480 real-time PCR machine (Roche Life Science, Penzberg, Germany) was used to quantify the abundance of selected genes related to the antioxidant defense system. The qRT-PCR reaction was set up by adding 10 μL 1× Power SYBR Green I (Bio-Rad, Hercules, CA) master mix, 0.3 μM of forward and reverse gene-specific primers, 7.4 μL deionized water and 2 μL first-strand cDNA template. The thermal cycling conditions were 3 min at 95 °C followed by 40 cycles of 15 s at 95 °C and 1 min at 60 °C. Comparative CT ($2^{-\Delta\Delta CT}$) method was employed to analyze the relative expression of each mRNA. Using sequence-specific primers, a total of 6 genes namely nuclear factor erythroid 2–related factor 2 (*NRF2*), Kelch-like erythroid cell–derived protein (*KEAP1*), superoxide dismutase-1 (*SOD1*), peroxiredoxin1 (*PRDX1*), thioredoxin-1 (*TXN1*) and catalase (*CAT*) were examined for their expression in GCs. GAPDH was used as an endogenous control to normalize the expression value. The primers were designed using primer3web version 4.0.4 (http://bioinfo.ut.ee/primer3/) and the sequences are listed in Supplementary Table S1.

Profiling and expression analysis of miRNAs

The miRNA expressions in the cells of the control and OS groups were performed using a ready-to-use miRNA PCR panel containing 84 mature miRNAs specific to apoptosis (MISH-114Z, Qiagen) following the manufacturer's instruction. In order to find the miRNA homology between human and bovine, we performed a comparative sequence analysis of 84 miRNAs in an array plate using miRBase 21 (http://www.mirbase.org/). The result showed 65 miRNAs to be completely identical with the bovine sequence, while 11 miRNAs have 1 nucleotide addition or deletion at 3′ or 5′ regions, 4 miRNAs have 1–5 nucleotide mismatch and no bovine sequence was detected for 4 miRNAs. The real-time PCR was run on a Roche Light cycler 480 real-time PCR machine (Roche Life Science, Penzberg, Germany) using the following thermal cycling parameters: 95 °C for 15 min, 40 cycles of 94 °C for 15 s, 55 °C for 30 s, 70 °C for 30 s followed by a melting curve analysis. A web-based PCR array data analysis software (http://pcrdataanalysis.sabiosciences.com/pcr/arrayanalysis.php) was used to analyze the PCR data. Data were normalized using the normalizer miRNAs present in the PCR plate. To avoid potential noise, miRNAs with a C*p* value higher than 35 were discarded from the list.

Target prediction and pathway analysis

To predict the potential targets of differentially regulated miRNAs, we used miRDB (http://www.mirdb.org/) and TargetScans (http://www.targetscan.org/vert_71/) web-based miRNA target prediction algorithms. Because all the differentially regulated miRNAs are completely identical in bovine and human, we obtained the target gene list using the human database. For visualization, annotation and pathway distribution, predicted target genes were uploaded to the DAVID Bioinformatics Resource (http://david.abcc.ncifcrf.gov/) server. The Kyoto Encyclopedia of Genes and Genomes (KEGG) database (http://www.genome.jp/kegg/) was used to represent the pathways.

Statistical analysis

All experiments were performed a minimum of three times. All the statistical analysis and graph preparation were performed using either IBM SPSS Statistics 23.0 or Microsoft Excel 2016 or GraphPad Prism software. Student's *t* test was used to detect a difference when two groups were compared. A difference between results was considered significant when the p value ≤ 0.05. Data are expressed as mean ± SEM of replicates.

Results

Characterization of OS in GCs

To confirm whether the expressions of miRNAs in GCs are truly changed due to OS, we first characterized OS in GCs. For this, GCs were grown and stimulated with 150 μM H_2O_2 for 4 h to develop a cell model of OS. GCs in both control and OS groups were examined after 4 h of culture period using an inverted microscope for the morphological changes. The morphometric observation confirms that the cells in the OS group showed typical signs of stress characterized by shrinkage in size, a lower number of live cells and a higher number of dead cells compared to the control (Fig. 1a, b). The results of cell viability, using the trypan blue exclusion test, showed that there was a significant ($p < 0.001$) loss cell viability (more than 50%) in the cells of the OS group compared to those of the untreated control group (Fig. 1c), which further indicates the presence of excessive stress. In addition, the results of the cell survival assay (cytotoxicity test) strengthen the findings of the morphometric observation and viability test as it also showed a lower number of viable cells in H_2O_2-treated cells compared to those of untreated cells indicated by a significantly ($p < 0.01$) lower absorbance value (Fig. 1d).

Following our observation of the morphologic changes and the decrease in the cell survival due to H_2O_2 stimulation, next, we sought to investigate differences in the generation of ROS molecules in the control and H_2O_2-treated groups as excessive production of ROS is the hallmark of OS. To quantify ROS, we used H_2DCFDA, which is a fluorogenic dye that can measure ROS within the cell. Upon diffusion into the cells, it is deacetylated by cellular esterases to a non-fluorescent compound, which is later oxidized by ROS to a highly fluorescent compound that can be detected by fluorescence microscopy. Administration of 150 μM H_2O_2 for 4 h resulted in a higher accumulation of ROS in cells, which is evidenced by the higher fluorescence intensity (Fig. 1e, f) and the histogram analysis of fluorescence intensity across the image revealed that the mean fluorescence intensity increased significantly ($p < 0.001$) in the OS group compared to the untreated control (Fig. 1g).

Under OS condition, the cytoplasmic NRF2 typically translocate to the nucleus in order to start the transcription of a battery of antioxidant enzymes that eventually scavenges the excessive ROS. Keeping this fact in mind, we next investigated the location of NRF2 in both the untreated control and OS groups using the immunocytochemistry technique. The results showed that NRF2 was predominantly located in the cytoplasm in the cells of the untreated control group (Fig. 1h), while almost all the NRF2 were translocated in the nucleus in the OS group (Fig. 1i).

OS impairs mitochondrial activity in GCs

To assess the effects of excessive ROS generated by H_2O_2 exposure, mitochondrial activity was determined and is presented in Fig. 2(a–d). Mitochondrial activity was dramatically decreased in the cells exposed to 150 μM H_2O_2 compared to that of the cells of the control group, which is evidenced by lower fluorescence activity in H_2O_2-exposed cells (Fig. 2a–c). Quantification of fluorescence intensity by ImageJ revealed that mean fluorescence intensity was significantly increased in the H_2O_2-treated cells compared to that of the untreated control (Fig. 2d).

OS-induced apoptosis in primary culture of GCs

To further investigate the effects of H_2O_2 in inducing OS-modulated cellular apoptosis in GCs, the fragmented DNA was detected in situ by TUNEL assay. The positively stained nuclei from randomly selected five fields were counted and the results were expressed as % positive nuclei/total nuclei ± SEM. As shown in Fig. 2(e–g), very few TUNEL-positive nuclei (0.8%) were detected in the untreated control group. However, a significantly higher ($p < 0.001$) number of TUNEL-positive cells (39%) were detected in H_2O_2-induced OS group (Fig. 2f, g) suggesting the treatment with H_2O_2-induced apoptosis in GCs.

OS modulates the expression of antioxidant genes

To confirm whether OS induced the expression of antioxidant genes, we checked the expression of the central genes of the Nrf2 pathway and candidate antioxidant genes. The result showed that the expression of both the NRF2 and candidate antioxidant genes was significantly ($p \leq 0.05$) increased in the GCs treated with H_2O_2 compared to that of the control (Fig. 3a–f). The expression of *KEAP1* (a negative regulator of *NRF2*) was significantly downregulated in the H_2O_2-treated GCs. These results further confirm the induction of strong OS due to the exposure of 150 μM H_2O_2.

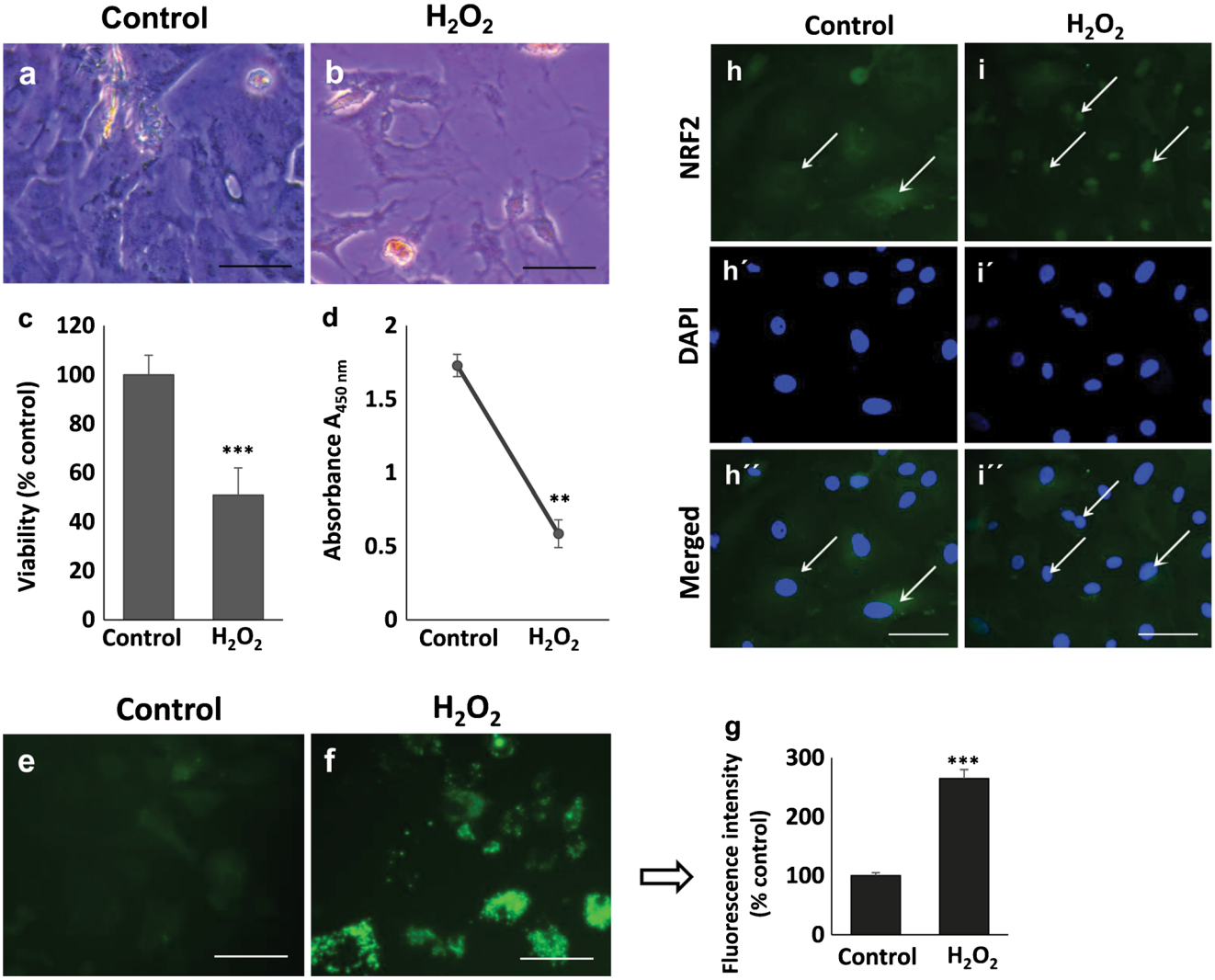

Fig. 1 Characterization of OS in GCs. GCs were isolated and cultured up to 40–50% confluence and treated with 150 μM H_2O_2 for 4 h to induce OS. OS was characterized by different morphological and molecular observations. (a) Microscopic picture of control and treated cells. (b) Cell viability determined by trypan blue exclusion test. (c) Cell proliferation was examined using WST-1 cell proliferation kit. (d, f) Accumulation of ROS determined by H_2DCFDA kit using fluorescence microscopy. Fluorescence intensity was quantified using the ImageJ program. (e) Visualization of nuclear translocation of the NRF2 protein. ImageJ software was used when mean fluorescence intensity was calculated. Scale bars, 100 μm. Experiments were performed in triplicate; data are presented as mean ± SEM; $^{**}p < 0.01$ and $^{***}p < 0.001$

Number of detected miRNAs

To understand whether OS modulation of miRNA abundance plays a role in GC apoptosis, the expression of miRNAs in GCs was quantified by ready-to-use 96-well PCR plates (Qiagen, Hilden) containing 84 mature human miRNAs related to apoptosis (either pro-apoptotic or anti-apoptotic) and 12 endogenous controls. The presence of miRNAs was determined based on crossing point (Cp) value and the % of detection within the replicates. miRNAs were considered detected when their Cp values were less than 35 and present in three replicates. The Cp value was set based on our previous experiences in detecting miRNAs in the qPCR array–based platform (Sohel et al. 2013; Noferesti et al. 2015). Of the 84 miRNAs investigated, a total of 63 miRNAs were detected in the cells of the control group, while 69 miRNAs were detected in the cells of the OS group. There are at least 6 miRNAs that were detected only in the cells of the OS group.

Differential expression of miRNAs in GCs exposed to OS

We next tested our hypothesis whether OS modulates the expression of miRNAs in GCs. Expression of miRNAs in the cells of the OS and control groups was analyzed using web-based miScript miRNA PCR Array Data analysis software provided by SABiosciences. Among the 69 miRNAs that

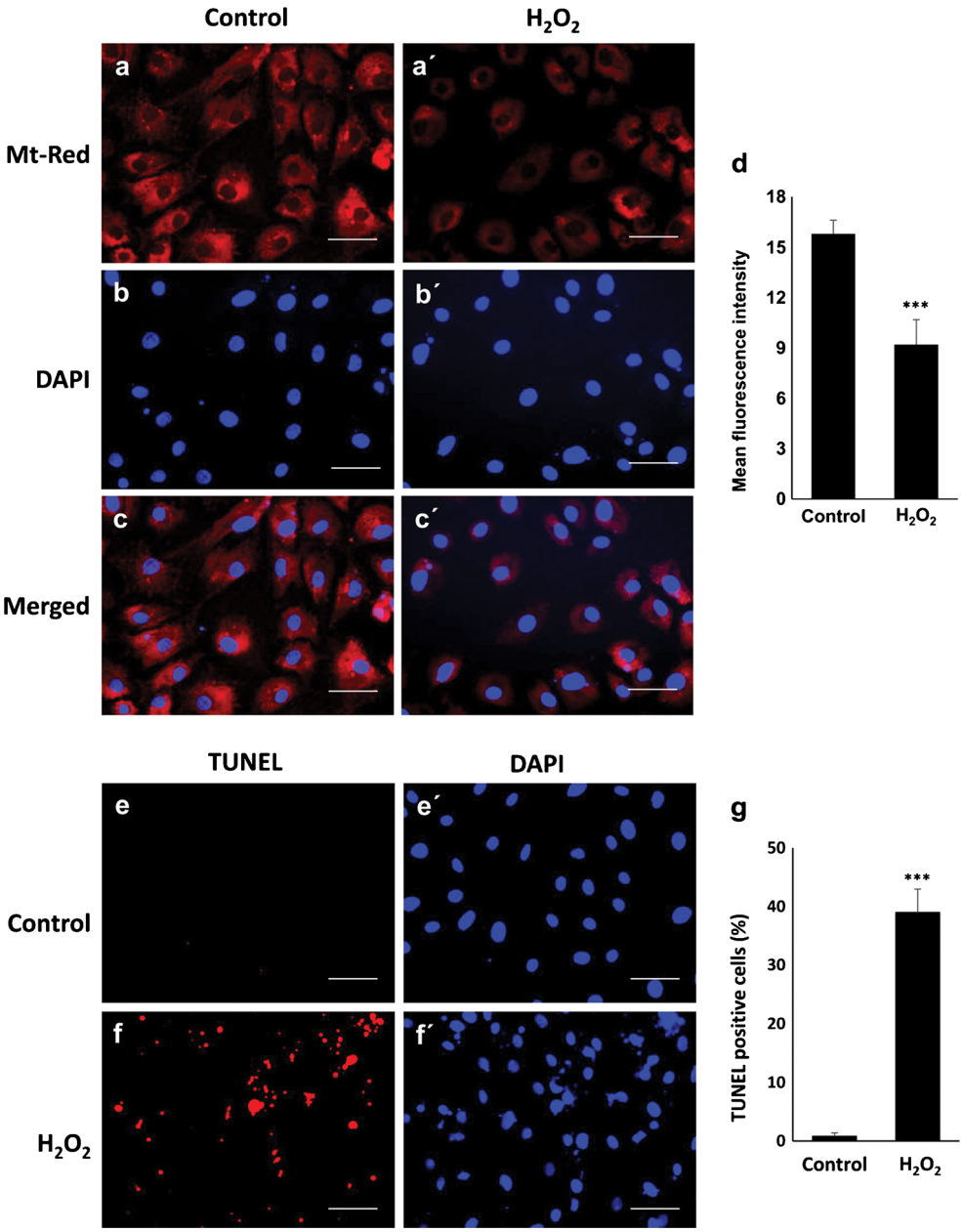

Fig. 2 Mitochondrial activity and apoptosis detection. GCs were grown and treated according to the experimental plan. (a) After the treatment period, the activity of mitochondria was detected using MitoTracker1 red fluorescence–based dye. Images were acquired with a fluorescence microscope using a red filter. (b) Fragmented DNA was detected by TUNEL assay and simultaneous nuclear staining with DAPI. Approximately 10,000 viable GCs were seeded in each well of a 96-well plate (flat bottom, tissue culture treated) and grown up to 50–60% confluence and treated according to the experimental plan. The results of the TUNEL assay showed that 150 μM H_2O_2 significantly increased the number of TUNEL-positive apoptotic nuclei after 4 h of incubation, whereas significantly less TUNEL-positive cells were observed in the untreated control. Scale bars, 100 μm. Experiments were performed in triplicate; data are presented as mean ± SEM; *** = $p < 0.001$. Mean fluorescence intensity was calculated using ImageJ software

were expressed in the cells of the OS group, a total of 47 miRNAs were upregulated in which 16 miRNAs including miR-365b-3p, miR-26b-5p, let-7c-5p, miR-143-3p and miR-29a-3p were upregulated with a fold change ranging from 2 to 18 (Table 1). On the other hand, among the 22 downregulated miRNAs, a total of 10 miRNAs including miR-210-3p, miR-145-5p, miR-378a-3p, miR-98-5p and miR-221-3p were downregulated with a range of 2–10-fold (Table 1). Sequence similarity check between human and bovine miRNAs revealed that hsa-miR-512-5p has no reported similar sequence in the bovine genome. Therefore, we discarded this miRNA from our list for further analysis. Among the upregulated miRNAs, miR-365b-3p showed the highest fold change regulation, whereas miR-210-3p showed the highest fold change regulation among downregulated miRNAs (Table 1).

Target prediction and functional annotation of target genes regulated by OS-modulated miRNAs

To identify the biological processes affected by deregulated miRNAs, we performed enrichment analysis on predicted target genes. TargetScan and miRDB algorithms were used to obtain the list of genes predicted to be targeted by the differentially expressed miRNAs. All the individual gene lists for both upregulated and downregulated miRNAs were merged and subsequently, duplicate values were removed from the merged list. A total of 6210 and 3575 genes were found to

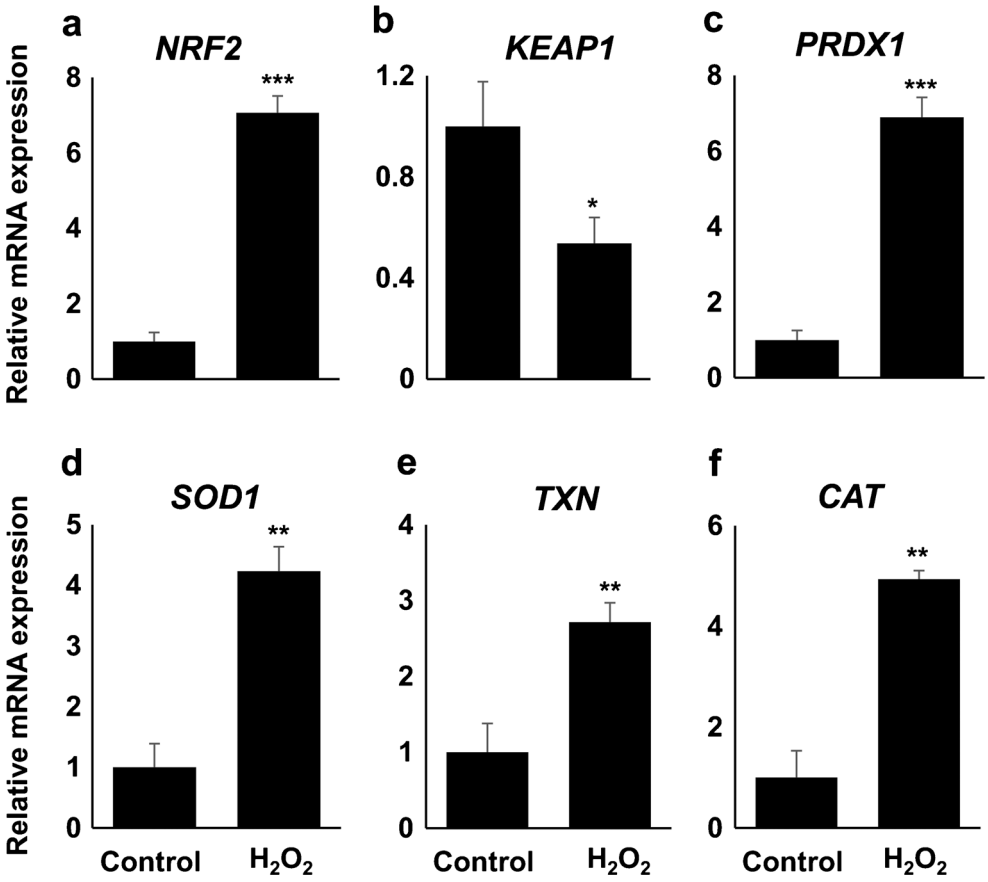

Fig. 3 Expression of *NRF2* and candidate antioxidant genes. Expression of *NRF2*, *KEAP1* and candidate genes downstream to NRF2 activation was quantified using qRT-PCR; relative abundance was analyzed using the comparative CT ($2^{-\Delta\Delta CT}$) method. Data are presented as mean ± SD of three biological replicates. Different asterisks represent statistically significant differences where $*p \leq 0.05$, $**p \leq 0.01$ and $***p \leq 0.001$ as determined by Student's *t* test

be affected by the upregulated and downregulated miRNAs, respectively. Detailed information about the number of target genes predicted to be targeted by individual miRNA in both up- and downregulated miRNAs are listed in Table 2 and Table 3, respectively.

To overcome the limitation of DAVID Bioinformatics tool, a maximum of 3000 genes processing ability in a single attempt, the top 250 genes were considered from each miRNA target gene list. Subsequently, we found 2892 genes and 1692 genes to be targeted by the upregulated and downregulated miRNAs, respectively. The gene lists were uploaded to the DAVID Bioinformatics database to identify significantly enriched canonical pathways. The results of the pathway analysis provided by the Kyoto Encyclopedia of Genes and Genomes (KEGG) showed that upregulated miRNAs are targeting the genes involved mostly in cell survival, intracellular communication and homeostasis cellular migration and growth control and disease pathways such as the PI3K-Akt signaling pathway, platelet activation, focal adhesion and the mTOR signaling pathway (Table 4). Among the pathways, the PI3K-Akt signaling pathway is one of the most significant pathways to be affected by the genes targeted by upregulated miRNAs. On the other hand, pathways involved in diseases like cancer, chronic myeloid leukemia, hepatitis B and pathways related to different signaling including the MAPK signaling pathway, Rap1 signaling pathway, thyroid hormone signaling pathway and FoxO signaling pathways were affected by the downregulated miRNAs (Table 5).

Discussion

A higher accumulation of inflammatory cells (neutrophils, vascular endothelial cells and macrophages) at the site of follicular rupture suggests that GCs are exposed to an elevated level of ROS during ovulation. In addition to metabolic sources, ROS contribution from external sources could make the situation more complex. Mammalian cells always integrate and respond to stress stimuli to decide cell fates whether to survive or die on a continuous basis. Several genes and signaling pathways are involved in this decision-making. As a master regulator of gene expression, miRNAs may play a significant role in this very complex mechanism. However, the role of miRNAs in OS-induced GC apoptosis is poorly understood. In the current experiment, we used 150 μM H_2O_2 for a 4-h exposure period to induce OS in GCs. Although GCs were collected from preovulatory large follicles, they maintain GC properties not luteinizing GCs. The concentration and the exposure time were adopted from a parallel experiment in our lab (data not shown). In one of our previous experiments, we

Table 1 List of differentially regulated miRNAs due to OS in GCs

Name of the miRNA	Fold change (control vs. treatment)	*p* value
miR-365b-3p	18.15	0.011439
miR-26b-5p	14.69	0.001867
let-7c-5p	6.67	0.003948
miR-143-3p	5.75	0.000003
miR-29a-3p	4.49	0.007341
miR-204-5p	4.02	0.005066
miR-16-5p	4	0.020813
miR-206	3.61	0.035981
miR-409-3p	3.42	0.020641
miR-149-3p	3.33	0.000002
miR-128-3p	3.06	0.009743
miR-25-3p	2.83	0.003128
miR-181a-5p	2.8	0.015152
miR-708-5p	2.67	0.015844
miR-125a-5p	2.34	0.000002
miR-153-3p	2.23	0.000042
miR-141-3p	− 2.18	0.012844
miR-92a-3p	− 2.29	0.011760
miR-186-3p	− 2.95	0.050975
miR-125b-5p	− 3.27	0.013494
miR-106b-5p	− 3.32	0.031496
miR-221-3p	− 5.47	0.012695
miR-98-5p	− 6.01	0.000263
miR-378a-3p	− 7.27	0.004742
miR-145-5p	− 9.43	0.002325
miR-210-3p	− 9.91	0.009260

used a comparatively higher concentration (500 μM H_2O_2) for a comparatively shorter exposure period (40 min) to induce OS in GCs (Sohel et al. 2018) where our main objective was to investigate the protective effects of sulforaphane against oxidative insult. However, in the current study, we used a comparatively lower concentration of H_2O_2 with a longer exposure period as our main objective was to investigate the OS modulation of apoptosis-associated miRNAs in GCs. We believe these conditions allowed a slower induction of OS and GCs had enough time to have a fate-making decision using molecular changes. A four-hour exposure with 150 μM H_2O_2 resulted in typical characteristics of OS including loss of cell viability, higher ROS accumulation and nuclear translocation of NRF2 in GCs. In addition, transcriptomic abundance of genes related to the antioxidant pathway was significantly increased in the GCs of OS group compared to that of control. The measurement of cellular apoptosis by TUNEL assay further suggests that the dramatic loss of cell viability may be due to cellular apoptosis mediated by H_2O_2-induced OS. In addition, miRNA expression analysis revealed that there was a massive deregulation of miRNA expression in the cells of the OS group and, most importantly, these miRNAs involved in several pathways may dictate several pathophysiological processes and the fate of the GCs.

Despite the fact that the physiological level of ROS plays a crucial role in reproductive processes, including follicular development, maturation of oocyte, luteal regression and fertilization (Agarwal et al. 2005; Shkolnik et al. 2011), a consistently higher accumulation of ROS, resulting OS, is considered one of the major stress inducers that significantly contributes to the fate of reproductive cells. Research has shown that OS not only induces a number of diseases including polycystic ovarian syndrome, endometritis and unexplained infertility, but also causes different pregnancy-related complications such as preeclampsia, recurrent pregnancy loss and spontaneous abortion (Agarwal et al. 2012). In a previous study, we showed that long-term exposure to a higher level of ROS results in characteristic cellular responses such as loss of cell viability, shrinking in size, mitochondrial damage, higher ROS accumulation and finally cell death in follicular GCs (Sohel et al. 2017). In the current study, we found that exposure to 150 μM H_2O_2 for 4 h resulted in a shrinkage in size of GCs and a higher accumulation of ROS accompanied by a significant loss of mitochondrial activity. Although the leakage of the mitochondrial electron transport chain is the major source of intracellular ROS, it could also be easily targeted by ROS. Furthermore, a damaged mitochondrion may produce higher ROS through its partially active electron transport chain. Under OS condition, an elevated level of ROS signals the breakdown of NRF2-KEAP1 bonding; thus, NRF2 translocates to the nucleus and activates the production of an array of antioxidant enzymes to neutralize the effect of excess ROS. In situ localization of NRF2 revealed that NRF2 was predominantly detected in the nucleus under stress conditions (Fig. 1i). It is highly likely that the concentration of H_2O_2 was highly cytotoxic and GCs were facing extreme OS. Therefore, the loss of GC viability in our study could be the result of higher levels of extracellular environmental ROS together with an intracellular source that subsequently causes a damage to cellular macromolecules, decreases proliferation and leads to cellular apoptosis.

The association of miRNAs with physiological processes and diseases has been reported in the context of potential involvement in diseases or developmental processes via their expression pattern or function. They are found to be involved in almost all events that took place in a female reproductive system including follicular development (Sontakke et al. 2014) and GC proliferation and function (Yao et al. 2010; Carletti et al. 2010; Yan et al. 2012; Yin et al. 2014). It has also been shown that several miRNAs are involved in OS-induced diseases (Sangokoya et al. 2010; Li et al. 2016), senescence and apoptosis (Magenta et al. 2011), cell survival (Cheng et al. 2009) and cell death (Thulasingam et al. 2011) in many cell types. However, a functional link between miRNA expression and OS in GCs remains to be investigated

Table 2 List of a total number of target genes and the name of top 10 genes predicted by upregulated miRNAs

Name of the microRNA	Number of genes	Official symbol of top 10 genes
miR-365b-3p	278	SGK1, HHIP, USP33, NR1D2, DLAT, UBAC2, UBP1, TIAM2, ZC3HAV1, UNC5D
miR-26b-5p	518	SLC2A13, SLC7A11, FAM98A, SLC45A4, ZDHHC6, PITPNC1, STRADB, RNF6, ZNF608, USP9X
let-7c-5p	435	SMARCAD1, FAM178A, LIN28B, GATM, LRIG3, GNPTAB, BZW1, ZNF322, ADAMTS8, C8orf58
miR-143-3p	375	GXYLT1, VASH1, ITM2B, ATP10A, IGFBP5, MSI2, ATP6V1A, MOGS, DENND1B, DIP2B
miR-29a-3p	632	BRWD3, COL3A1, ERCC6, DGKH, ATAD2B, FBN1, NFIA, TET3, NAV3, ROBO1
miR-204-5p	599	C9orf72, RAB22A, AP1S2, ANKRD13A, EBF2, ACSL4, ZNF423, PTPRD, SASS6, SPRED1
miR-16-5p	1089	ZFHX4, SYNJ1, SLC9A6, IPO7, CDCA4, NUP50, PAPPA, LUZP1, SLC13A3, UNC80
miR-206	417	PTPLAD1, GLCCI1, LPPR4, ZMAT3, TPPP, CDK14, ANKRD29, EIF4E, NRP1, C2orf69
miR-409-3p	258	KIAA2022, YTHDF3, NXPH1, SLC35A3, KLF15, OXR1, CPSF6, RAB10, ZDHHC20
miR-149-3p	1461	NFIX, C20orf96, SSBP3, HCFC1, SPRY4, SOX13, NACC1, PVRL1, AR, RAB5B
miR-128-3p	625	PAIP2, SZRD1, NFX1, POGLUT1, EFR3A, BAG2, AK2, SEC22A, LBH, TRIL
miR-25-3p	496	DNAJB9, CD69, SYNJ1, FBXW7, SLC12A5, EFR3A, MAP 2K4, USP28, KIAA1109, KIAA1432
miR-181a-5p	887	C2CD5, FIGN, S1PR1, PDE5A, MTMR12, TBC1D1, TNPO1, PROX1, OSBPL3, MICU3
miR-708-5p	277	GPM6A, PAPPA, FAM107A, TNS3, TEF, HOXA1, KIAA0355, FOXJ3, JPH1, EN2
miR-125a-5p	479	IRF4, LACTB, OSBPL9, ZSWIM6, ENPEP, HIF1AN, GCNT1, SLC39A9, SMEK1, SEMA4D
miR-153-3p	365	YIPF2, SLC4A4, OSBPL6, EBF2, NFE2L2, PLCB1, NAV2, RAI14, DMD, UTRN
miR-512-5p	242	BAZ2A, ATRX, PHF6, HLTF, CENPL, TBL1XR1, PRR14L, HSPA12A, DDX6, SRPK2

as very little is known about OS modulation of miRNA expression in GCs, which may be a contributing factor in the progression of any unexplained pathological condition. In the present study, we investigated the expression of 84 mature miRNAs related to apoptosis and the result confirms that there was a massive deregulation of miRNA expression in GCs due to OS. It is interesting to note that the number of upregulated miRNAs was higher than the number of downregulated miRNAs. This is may be due to the fact that the PCR array contains a higher number of pro-apoptotic miRNAs than anti-apoptotic miRNAs and incubation of GCs with 150 μM H_2O_2 for 4 h may induce incredible OS to the cells that modulate the higher expression of apoptosis-associated miRNAs.

Among the upregulated miRNAs, miR-365b-3p, miR-26b-5p and let-7c-5p are the top three upregulated miRNAs. Previous studies have shown that several of these miRNAs are involved in proliferation, growth, cell cycle arrest and apoptosis. For instance, higher expression of miR-365b-3p significantly attenuates cell growth and induces cell cycle arrest and apoptosis in human retinoblastoma cells (Wang et al. 2013) and hepatocellular carcinoma cells (Li et al. 2017). Overexpression of miR-26b-5p was reported as a regulator of cell cycle, proliferation and migration (Du et al. 2015) and an important inducer of apoptosis in different cell types including porcine ovarian GCs (Liu et al. 2016). Although let-7c-5p is not directly involved in the process of stress-induced apoptosis, it is protecting the brain against cerebral ischemia injury (Ni et al. 2015) and the higher expression of let-7c-5p in our experiment may be due to the fact that this miRNA is highly abundant in reproductive tissues that were previously reported (Li et al. 2011). It has been shown that overexpression of miR-128a and miR-181a promotes apoptosis in mouse

Table 3 List of a total number of target genes and the name of the top 10 genes predicted by downregulated miRNAs

Name of the microRNA	Number of genes	Official symbol of top 10 genes
miR-210-3p	39	FGFRL1, ISCU, RRP1B, DENND6A, IGF2, ZNF462, DHX58, KMT2D, CORO2B, ACVR1B
miR-145-5p	495	ABCE1, MPZL2, DAB2, KCNA4, ABHD17C, AP1G1, YTHDF2, SPSB4, ATP8A1, SEMA3A
miR-378a-3p	169	NR2C2, KIAA1522, TMEM245, SLC7A6, MPP3, RAB10, SERINC1, NKX3-1, FLT1, ELAC1
miR-98-5p	437	SMARCAD1, LIN28B, FAM178A, GNPTAB, LRIG3, GATM, ADAMTS8, DNA2, ADRB2, BZW1
miR-221-3p	316	GABRA1, PANK3, TCF12, CDKN1B, HECTD2, RFX7, TMCC1, FNDC3A, ARF4, C3orf70
miR-106b-5p	855	PTPN4, ARID4B, EPHA4, PKD2, PDCD1LG2, SLC40A1, FBXL5, ZNF800, ADARB1, ZNFX1
miR-125b-5p	476	IRF4, ZSWIM6, ENPEP, LACTB, OSBPL9, GCNT1, HIF1AN, IER3IP1, SEMA4D, SLC39A9
miR-186-3p	551	MAML2, MYCBP, HLCS, RAB11FIP1, KDM2A, HMBOX1, LIN54, TMEM181, UBE2Q1, BCL6
miR-92a-3p	496	SYNJ1, DNAJB9, EFR3A, SLC12A5, USP28, FBXW7, CD69, APPL1, MOAP1, MAP 2 K4
miR-141-3p	759	DUSP3, TMEM170B, ZBTB34, DCP2, ATP8A1, MYBL1, ZEB2, TRHDE, HS2ST1, ELAVL2

Table 4 Top 10 pathways predicted to be targeted by the upregulated miRNAs after H_2O_2 stimulation

Pathway name	miRNAs involved	Targets in the pathway	*p* value	Top predicted genes in the pathway
PI3K-Akt signaling pathway	miR-16-5p, miR-25-3p, miR-29a-3p, miR-143-3p, miR-149-3p, miR-153-3p, miR-181a-3p, miR-365b-3p,	63	4.32×10^{-10}	HRAS, FGF7, FGF9, PDGFA, FGF17, EFNA3, RPS6KB1, FOXO3, PTEN, CCNE1
Platelet activation	miR-25-3p, miR-29a-3p, miR-365b-3p,	36	2.48×10^{-7}	GNA13, GNAI3, ADCY2, ADCY6, COL3A1, COL2A1, ITGB3, PLCB4, FGB, PPP1R12A
Focal adhesion	miR-16-5p, miR-25-3p, miR-26b-5p, miR-29a-3p, miR-143-3p, miR-149-3p,	48	5.29×10^{-7}	CAV2, GRB2, COL3A1, COL2A1, ITGB3, PTEN, CTNNB1, IGF1R, PAK2, ITGB8
mTOR signaling pathway	miR-16-5p, miR-26b-5p, miR-29a-3p, miR-149-3p, miR-181a-3p,	20	6.64×10^{-6}	PIK3CB, IGF1, RPS6KB1, RICTOR, IRS1, PTEN, RPS6KA6, MAPK1, EIF4EBP1, EIF4E
Prostate cancer	miR-29a-3p, miR-149-3p, miR-181a-3p, miR-365b-3p,	25	1.52×10^{-5}	E2F2, GRB2, PTEN, CTNNB1, CCNE1, IGF1R, KRAS, SOS1, CREB3L2, NKX3-1
Neurotrophin signaling pathway	miR-16-5p, miR-29a-3p, miR-143-3p, miR-149-3p, miR-181a-3p, miR-204-5p, miR-708-5p	30	2.61×10^{-5}	GRB2, BDNF, KRAS, MAP 3K3, SOS1, MAP 3K1, GAB1, CAMK2D, CAMK2B, PIK3R5
Axon guidance	miR-26b-5p, miR-149-3p, miR-153-3p, miR-204-5p, miR-206, miR-708-5p	31	3.04×10^{-5}	DCC, PLXNC1, GNAI3, NRP1, PLXNA2, PPP3R1, SEMA5A, EPHB6, KRAS, PAK2
Signaling pathways regulating pluripotency of stem cells	miR-16-5p, miR-29a-3p, miR-149-3p, miR-708-5p	33	3.37×10^{-5}	SMARCAD1, WNT5B, GRB2, PAX6, REST, ZIC3, ACVR1C, CTNNB1, IGF1R, PCGF3
Insulin signaling pathway	miR-16-5p, miR-29a-3p, miR-149-3p,	32	6.35×10^{-5}	GRB2, PHKA1, MKNK2, RHOQ, RPS6KB1, PPP1R3D, PRKAR2A, EIF4EBP1, KRAS, SOS1
ErbB signaling pathway	miR-16-5p, miR-29a-3p, miR-149-3p, miR-708-5p	23	1.19×10^{-4}	GRB2, PIK3CB, CBL, MAP 2K4, RPS6KB1, MAPK1, NRAS, EIF4EBP1, CDKN1A, KRAS

GCs and are positively regulated by H_2O_2-induced OS (Wang et al. 2016; Zhang et al. 2017a). In our experiment, we found both the miRNAs are significantly upregulated in bovine GCs treated with H_2O_2. On the other hand, top downregulated miRNAs, such as miR-210-3p, miR-145-5p and miR-378a-3p, are known as hypoxamiRs and anti-tumor miRNAs and exhibit anti-apoptotic effects and regulate multiple cellular pathways. miR-210 is shown to be involved in the modulation of endothelial cell responses under hypoxia and expression of miR-210 progressively increased upon exposure to hypoxia (lower level of oxygen molecules) (Fasanaro et al. 2008). On the other hand, exposure to hyperoxia could lead to increased generation of ROS molecules in cells and vice versa. Therefore, in our study, the lower expression of miR-210 could be the result of H_2O_2-induced higher production of ROS that may lead to hyperoxic conditions in GCs. It is well known that miR-145 plays a key role as a tumor suppressor in many types of cancer (Cui et al. 2014). In addition, recently, Xu et al. (2017) showed that lower expression of miR-145 induces apoptosis in mouse GCs by targeting Krüppel-like factor 4 (KLF 4) in vitro. Furthermore, using an in vivo mouse model, the authors demonstrated that lack of miR-145 expression promotes apoptosis in GCs through upregulating KLF 4 (Xu et al. 2017). In agreement with these findings, in our study, we found that miR-145 was significantly downregulated in the GCs of the OS group compared to that of the untreated control group indicating that the OS modulation of miRNA expression promotes GC apoptosis.

To identify the potential biological functions of significantly deregulated miRNAs due to H_2O_2 exposure, target mRNAs were predicted and enrichment analysis of multiple miRNA target genes was performed by KEGG. The most significantly enriched pathways predicted to be targeted by the upregulated miRNAs are the PI3K-Akt signaling pathway, platelet activation, focal adhesion, mTOR signaling pathway, prostate cancer, neurotrophin signaling pathway and axon guidance. Many of these pathways are known to be involved in different cellular signaling including cell proliferation, cell migration, cell survival and apoptosis. For instance, the PI3K-Akt signaling pathway has been shown to be directly involved in the survival of induced pluripotent stem cells (Hossini et al. 2016) and delivers anti-apoptotic signals (Kennedy et al. 1997). In addition, it has been shown that activation of PI3K-Akt effectively inhibits the apoptosis

Table 5 List of top 10 enriched pathways that are predicted to be targeted by the downregulated miRNAs

Pathway name	miRNAs involved	Targets in the pathway	*p* value	Top predicted genes in the pathway
Proteoglycans in cancer	miR-92a-3p, miR-106b-5p, miR-141-3p, miR-221-3p	39	6.88×10^{-7}	FZD10, PIK3CB, ROCK2, FZD3, EGFR, TIAM1, GAB1, ESR1
MAPK signaling pathway	miR-106b-5p, miR-141-3p, miR-221-3p	45	1.47×10^{-6}	FGF5, ZAK, MAP 3K5, IRS2, CREB1, PRKAB1, FOS, NTF3, MAP 3K2
Endocytosis	miR-106b-5p, miR-141-3p, miR-378a-3p	36	1.17×10^{-5}	RAB5B, LDLR, TSG101, SNX4, ARF6, EEA1, VPS37C, KIT, ARPC5, SRC, TGF
Rap1 signaling pathway	miR-141-3p, miR-221-3p	24	3.83×10^{-5}	GNAI3, TLN2, FGF9, ITGB3, KIT, SRC, ACTG1, IGF1R, CNR1, RALB
Thyroid hormone signaling pathway	miR-106b-5p	56	4.21×10^{-5}	ACTB, KAT2B, PIK3CB, ATP1B4, ESR1, ITGB3, SRC, PRKCB, MED12L, ACTG1
Pathways in cancer	miR-92a-3p, miR-106b-5p, miR-141-3p, miR-221-3p, miR-378a-3p	18	5.12×10^{-5}	GNA13, E2F1, E2F2, FGF9, PTEN, CXCL12, TGFB2, CCNE2, FOS, SLC2A1
Chronic myeloid leukemia	miR-106b-5p, miR-141-3p	26	5.39×10^{-5}	E2F1, E2F2, BCR, GRB2, PIK3CB, TGFBR1, CBL, TGFBR2, TGFB2, NRAS
FoxO signaling pathway	miR-92a-3p, miR-106b-5p, miR-141-3p	27	7.76×10^{-5}	GRB2, FOXO4, CCNG2, PTEN, TGFB2, IGF1R, S1PR1, SOS1, BCL6, PIK3R5
Hepatitis B	miR-92a-3p, miR-106b-5p, miR-141-3p, miR-221-3p	17	1.12×10^{-4}	E2F1, E2F2, GRB2, TIRAP, PTEN, SRC, ATF2, TGFB2, CCNE2, FOS
Apoptosis	miR-16-5p, miR-25-3p, miR-149-3p, miR-153-3p, miR-181a-3p	18	3.36×10^{-4}	BID, TNF, PIK3CB, AIFM1, DFFB, RELA, CYCS, TP53, BCL2L1, TNFRSF1A

in GCs against OS induced by H_2O_2 (Nakahara et al. 2012). Activation of the focal adhesion pathway was shown to be a suppressor of apoptosis in normal epithelial and endothelial cells (Frisch et al. 1996). In addition, the mTOR signaling pathway is considered a conserved regulator of cell growth, proliferation and survival (Hung et al. 2012). On the other hand, pathways like proteoglycans in cancer, MAPK signaling pathway, endocytosis, Rap1 signaling pathway, thyroid hormone signaling pathway and FOXO signaling pathways were predicted to be affected by the downregulated miRNAs. In addition to steroid synthesis in GCs (Manna and Stocco 2011), the MAPK signaling pathway is the major pathway that is also involved in the modulation of gene expression, proliferation, mitosis, metabolism and mobility (Mebratu and Tesfaigzi 2009; Yang and Huang 2015). Studies have demonstrated that ROS can induce or mediate the activation of the MAPK pathways and scavenging of ROS by antioxidants blocks MAPK activation (Son et al. 2011), indicating a higher accumulation of ROS induced by H_2O_2 may downregulate the expression of specific miRNAs (miR-106b-5p, miR-141-3p, miR-221-3p), which is essential in the activation of the MAPK pathway. It has been reported that Ras-associated protein-1 (Rap1), a small GTPase in the Ras-related protein family, is an important regulator of basic cellular functions (e.g., formation and control of cell adhesion and junctions), cellular migration and polarization (Zhang et al. 2017b). The thyroid signaling pathway is closely related to the cellular antioxidant system and OS has been shown to be associated with both hyperthyroidism and hypothyroidism (Mancini et al. 2016). It has also been shown that the thyroid signaling pathway plays a crucial role in female reproduction including altering ovarian function (Wei et al. 2018), follicular development (Fedail et al. 2014) and preimplantation and early development of embryos (Colicchia et al. 2014). Pathway analysis of our study indicates that OS may modulate the expression of miRNAs in a manner that suppresses the activation of pathways related to cell survival and activates both pro-apoptotic pathways and pathways related to diseases.

In the present study, we demonstrated, for the first time, the OS modulation of miRNA expression in bovine ovarian GCs. Our results showed that a number of pro-apoptotic miRNAs including miR-365b-3p were upregulated while anti-apoptotic miRNAs including miR-210-3p were downregulated in response to OS. These two miRNAs can be considered markers for OS in GCs. Furthermore, pathway analysis revealed that several pathways related to cell proliferation, migration, apoptosis and survival were affected by deregulated miRNAs. Taken together, our study demonstrated that H_2O_2-induced OS impaired the cellular function and led to apoptosis by upregulating pro-apoptotic miRNAs and downregulating anti-apoptotic miRNAs. The results of the current study provoke us to speculate that OS at the time of ovulation causes cellular and molecular damages to GCs where miRNAs may play a central role. However, a functional study using the miRNA knockdown/mimic approach is required to validate the association of miRNA-mRNA interaction and the association of differentially expressed miRNAs with the predicted pathways.

Acknowledgments The authors are indebted to Res. Asst. Mahmut Kaliber; Sebahattin Koknur, DVM; and Ali Ergin, DVM, for their assistance during sample collection.

Funding This research was supported by the Erciyes University Scientific Research Projects Coordination Unit, Project No: FOA-2015-5655.

Compliance with ethical standards

Conflict of interest The authors declare that they have no conflict of interest.

Statement on the welfare of animals This article does not contain any studies with live animals performed by any of the authors.

Disclaimer The funders had no role in study design, data collection and analysis, decision to publish, or preparation of the manuscript.

Publisher's Note Springer Nature remains neutral with regard to jurisdictional claims in published maps and institutional affiliations.

References

Agarwal A, Gupta S, Sharma RK (2005) Role of oxidative stress in female reproduction. Reprod Biol Endocrinol 3(28). https://doi.org/10.1186/1477-7827-3-28

Agarwal A, Aponte-Mellado A, Premkumar BJ et al (2012) The effects of oxidative stress on female reproduction: a review. Reprod Biol Endocrinol 10:49. https://doi.org/10.1186/1477-7827-10-49

Al-Gubory KH, Fowler PA, Garrel C (2010) The roles of cellular reactive oxygen species, oxidative stress and antioxidants in pregnancy outcomes. Int J Biochem Cell Biol 42:1634–1650. https://doi.org/10.1016/J.BIOCEL.2010.06.001

Appasamy M, Jauniaux E, Serhal P et al (2008) Evaluation of the relationship between follicular fluid oxidative stress, ovarian hormones, and response to gonadotropin stimulation. Fertil Steril 89:912–921. https://doi.org/10.1016/J.FERTNSTERT.2007.04.034

Ávila J, González-Fernández R, Rotoli D et al (2016) Oxidative stress in granulosa-lutein cells from in vitro fertilization patients. Reprod Sci 23:1656–1661. https://doi.org/10.1177/1933719116674077

Carletti MZ, Fiedler SD, Christenson LK (2010) MicroRNA 21 blocks apoptosis in mouse periovulatory granulosa cells1. Biol Reprod 83:286–295. https://doi.org/10.1095/biolreprod.109.081448

Cheng Y, Liu X, Zhang S et al (2009) MicroRNA-21 protects against the H2O2-induced injury on cardiac myocytes via its target gene PDCD4. J Mol Cell Cardiol 47:5–14. https://doi.org/10.1016/J.YJMCC.2009.01.008

Colicchia M, Campagnolo L, Baldini E et al (2014) Molecular basis of thyrotropin and thyroid hormone action during implantation and early development. Hum Reprod Update 20:884–904. https://doi.org/10.1093/humupd/dmu028

Cui S-Y, Wang R, Chen L-B (2014) MicroRNA-145: a potent tumour suppressor that regulates multiple cellular pathways. J Cell Mol Med 18:1913–1926. https://doi.org/10.1111/jcmm.12358

Donadeu FX, Schauer SN, Sontakke SD (2012) Involvement of miRNAs in ovarian follicular and luteal development. J Endocrinol 215:323–334. https://doi.org/10.1530/JOE-12-0252

Du J-Y, Wang L-F, Wang Q, Yu L-D (2015) miR-26b inhibits proliferation, migration, invasion and apoptosis induction via the downregulation of 6-phosphofructo-2-kinase/fructose-2,6-bisphosphatase-3 driven glycolysis in osteosarcoma cells. Oncol Rep 33:1890–1898. https://doi.org/10.3892/or.2015.3797

Duffy DM, Stouffer RL (2003) Luteinizing hormone acts directly at granulosa cells to stimulate periovulatory processes: modulation of luteinizing hormone effects by prostaglandins. Endocrine 22:249–256. https://doi.org/10.1385/ENDO:22:3:249

Fasanaro P, D'Alessandra Y, Di Stefano V et al (2008) MicroRNA-210 modulates endothelial cell response to hypoxia and inhibits the receptor tyrosine kinase ligand Ephrin-A3. J Biol Chem 283:15878–15883. https://doi.org/10.1074/jbc.M800731200

Fedail JS, Zheng K, Wei Q et al (2014) Roles of thyroid hormones in follicular development in the ovary of neonatal and immature rats. Endocrine 46:594–604. https://doi.org/10.1007/s12020-013-0092-y

Frisch SM, Vuori K, Ruoslahti E, Chan-Hui PY (1996) Control of adhesion-dependent cell survival by focal adhesion kinase. J Cell Biol 134:793–799

Gonzalez G, Behringer RR (2009) *Dicer* is required for female reproductive tract development and fertility in the mouse. Mol Reprod Dev 76:678–688. https://doi.org/10.1002/mrd.21010

Hawkins SM, Andreu-Vieyra CV, Kim TH et al (2012) Dysregulation of uterine signaling pathways in progesterone receptor- *Cre* knockout of *Dicer*. Mol Endocrinol 26:1552–1566. https://doi.org/10.1210/me.2012-1042

Hong X, Luense LJ, McGinnis LK et al (2008) Dicer1 is essential for female fertility and normal development of the female reproductive system. Endocrinology 149:6207–6212. https://doi.org/10.1210/en.2008-0294

Hossain MM, Sohel MMH, Schellander K, Tesfaye D (2012) Characterization and importance of microRNAs in mammalian gonadal functions. Cell Tissue Res 349:679–690. https://doi.org/10.1007/s00441-012-1469-6

Hossini AM, Quast AS, Plötz M et al (2016) PI3K/AKT signaling pathway is essential for survival of induced pluripotent stem cells. PLoS One 11:e0154770. https://doi.org/10.1371/journal.pone.0154770

Hung C-M, Garcia-Haro L, Sparks CA, Guertin DA (2012) mTOR-dependent cell survival mechanisms. Cold Spring Harb Perspect Biol. https://doi.org/10.1101/cshperspect.a008771

Kennedy SG, Wagner AJ, Conzen SD et al (1997) The PI 3-kinase/Akt signaling pathway delivers an anti-apoptotic signal. Genes Dev 11:701–713. https://doi.org/10.1101/GAD.11.6.701

Li M, Liu Y, Wang T et al (2011) Repertoire of porcine microRNAs in adult ovary and testis by deep sequencing. Int J Biol Sci 7:1045–1055

Li J, Li J, Wei T, Li J (2016) Down-regulation of MicroRNA-137 improves high glucose-induced oxidative stress injury in human umbilical vein endothelial cells by up-regulation of AMPKα1. Cell Physiol Biochem 39:847–859. https://doi.org/10.1159/000447795

Li M, Yang Y, Kuang Y et al (2017) miR-365 induces hepatocellular carcinoma cell apoptosis through targeting Bcl-2. Exp Ther Med 13:2279–2285. https://doi.org/10.3892/etm.2017.4244

Liu J, Tu F, Yao W et al (2016) Conserved miR-26b enhances ovarian granulosa cell apoptosis through HAS2-HA-CD44-Caspase-3 pathway by targeting HAS2. Sci Rep 6:21197. https://doi.org/10.1038/srep21197

Magenta A, Cencioni C, Fasanaro P et al (2011) miR-200c is upregulated by oxidative stress and induces endothelial cell apoptosis and senescence via ZEB1 inhibition. Cell Death Differ 18:1628–1639. https://doi.org/10.1038/cdd.2011.42

Mancini A, Di Segni C, Raimondo S et al (2016) Thyroid hormones, oxidative stress, and inflammation. Mediat Inflamm 2016:6757154. https://doi.org/10.1155/2016/6757154

Manna PR, Stocco DM (2011) The role of specific mitogen-activated protein kinase signaling cascades in the regulation of steroidogenesis. J Signal Transduct 2011:821615. https://doi.org/10.1155/2011/821615

Mebratu Y, Tesfaigzi Y (2009) How ERK1/2 activation controls cell proliferation and cell death: is subcellular localization the answer? Cell Cycle 8:1168–1175. https://doi.org/10.4161/cc.8.8.8147

Nagaraja AK, Andreu-Vieyra C, Franco HL et al (2008) Deletion of Dicer in somatic cells of the female reproductive tract causes sterility. Mol Endocrinol 22:2336–2352. https://doi.org/10.1210/me.2008-0142

Nakahara T, Iwase A, Nakamura T et al (2012) Sphingosine-1-phosphate inhibits H2O2-induced granulosa cell apoptosis via the PI3K/Akt signaling pathway. Fertil Steril 98:1001–1008.e1. https://doi.org/10.1016/J.FERTNSTERT.2012.06.008

Ngamwongsatit P, Banada PP, Panbangred W, Bhunia AK (2008) WST-1-based cell cytotoxicity assay as a substitute for MTT-based assay for rapid detection of toxigenic Bacillus species using CHO cell line. J Microbiol Methods 73:211–215. https://doi.org/10.1016/j.mimet.2008.03.002

Ni J, Wang X, Chen S et al (2015) MicroRNA let-7c-5p protects against cerebral ischemia injury via mechanisms involving the inhibition of microglia activation. Brain Behav Immun 49:75–85. https://doi.org/10.1016/j.bbi.2015.04.014

Noferesti SS, Sohel MMH, Hoelker M et al (2015) Controlled ovarian hyperstimulation induced changes in the expression of circulatory miRNA in bovine follicular fluid and blood plasma. J Ovarian Res 8:81. https://doi.org/10.1186/s13048-015-0208-5

Pastorelli LM, Wells S, Fray M et al (2009) Genetic analyses reveal a requirement for Dicer1 in the mouse urogenital tract. Mamm Genome 20:140–151. https://doi.org/10.1007/s00335-008-9169-y

Peng Y, Croce CM (2016) The role of microRNAs in human cancer. Signal Transduct Target Ther 2016:1–9. https://doi.org/10.1038/sigtrans.2015.4

Ray PD, Huang B-W, Tsuji Y (2012) Reactive oxygen species (ROS) homeostasis and redox regulation in cellular signaling. Cell Signal 24:981–990. https://doi.org/10.1016/j.cellsig.2012.01.008

Romaine SPR, Tomaszewski M, Condorelli G, Samani NJ (2015) MicroRNAs in cardiovascular disease: an introduction for clinicians. Heart 101:921–928. https://doi.org/10.1136/heartjnl-2013-305402

Sangokoya C, Telen MJ, Chi J-T et al (2010) microRNA miR-144 modulates oxidative stress tolerance and associates with anemia severity in sickle cell disease. Blood 116:4338–4348. https://doi.org/10.1182/blood-2009-04-214817

Shkolnik K, Tadmor A, Ben-Dor S et al (2011) Reactive oxygen species are indispensable in ovulation. Proc Natl Acad Sci U S A 108:1462–1467. https://doi.org/10.1073/pnas.1017213108

Simpson K, Wonnacott A, Fraser DJ, Bowen T (2016) MicroRNAs in diabetic nephropathy: from biomarkers to therapy. Curr Diab Rep 16:35. https://doi.org/10.1007/s11892-016-0724-8

Sohel MMH (2016) Extracellular/circulating microRNAs: release mechanisms, functions and challenges. Achiev Life Sci 10:175–186. https://doi.org/10.1016/j.als.2016.11.007

Sohel MMH, Cinar MU (2015) Advancement in molecular genetics to understand the molecular reproduction of livestock – follicular development. Res Agric Livest Fish 1:47–60. https://doi.org/10.3329/ralf.v1i1.22355

Sohel MMH, Hoelker M, Noferesti SS et al (2013) Exosomal and non-exosomal transport of extra-cellular microRNAs in follicular fluid: implications for bovine oocyte developmental competence. PLoS One. https://doi.org/10.1371/journal.pone.0078505

Sohel MH, Cinar MU, Kalibar M et al (2016) Appropriate concentration of hydrogen peroxide and Sulforaphane for granulosa cells to study oxidative stress in vitro. J Biotechnol 231:S24. https://doi.org/10.1016/j.jbiotec.2016.05.104

Sohel MMH, Konca Y, Akyuz B et al (2017) Concentration dependent antioxidative and apoptotic effects of sulforaphane on bovine granulosa cells in vitro. Theriogenology 97:17–26. https://doi.org/10.1016/j.theriogenology.2017.04.015

Sohel MMH, Amin A, Prastowo S, et al (2018) Sulforaphane protects granulosa cells against oxidative stress via activation of NRF2-ARE pathway. Cell Tissue Res 1–13. https://doi.org/10.1007/s00441-018-2877-z

Son Y, Cheong Y-K, Kim N-H et al (2011) Mitogen-activated protein kinases and reactive oxygen species: how can ROS activate MAPK pathways? J Signal Transduct 2011:792639. https://doi.org/10.1155/2011/792639

Sontakke SD, Mohammed BT, McNeilly AS, Donadeu FX (2014) Characterization of microRNAs differentially expressed during bovine follicle development. Reproduction 148:271–283. https://doi.org/10.1530/REP-14-0140

Tesfaye D, Salilew-Wondim D, Gebremedhn S et al (2017) Potential role of microRNAs in mammalian female fertility. Reprod Fertil Dev 29:8–23. https://doi.org/10.1071/RD16266

Thulasingam S, Massilamany C, Gangaplara A et al (2011) miR-27b*, an oxidative stress-responsive microRNA modulates nuclear factor-kB pathway in RAW 264.7 cells. Mol Cell Biochem 352:181–188. https://doi.org/10.1007/s11010-011-0752-2

Wang J, Wang X, Wu G et al (2013) MiR-365b-3p, down-regulated in retinoblastoma, regulates cell cycle progression and apoptosis of human retinoblastoma cells by targeting PAX6. FEBS Lett 587:1779–1786. https://doi.org/10.1016/J.FEBSLET.2013.04.029

Wang C, Li D, Zhang S et al (2016) MicroRNA-125a-5p induces mouse granulosa cell apoptosis by targeting signal transducer and activator of transcription 3. Menopause 23:100–107. https://doi.org/10.1097/GME.0000000000000507

Wei Q, Fedail JS, Kong L et al (2018) Thyroid hormones alter estrous cyclicity and antioxidative status in the ovaries of rats. Anim Sci J 89:513–526. https://doi.org/10.1111/asj.12950

Xu L, Sun H, Zhang M et al (2017) MicroRNA-145 protects follicular granulosa cells against oxidative stress-induced apoptosis by targeting Krüppel-like factor 4. Mol Cell Endocrinol 452:138–147. https://doi.org/10.1016/J.MCE.2017.05.030

Yan G, Zhang L, Fang T et al (2012) MicroRNA-145 suppresses mouse granulosa cell proliferation by targeting activin receptor IB. FEBS Lett 586:3263–3270. https://doi.org/10.1016/j.febslet.2012.06.048

Yang M, Huang C-Z (2015) Mitogen-activated protein kinase signaling pathway and invasion and metastasis of gastric cancer. World J Gastroenterol 21:11673. https://doi.org/10.3748/wjg.v21.i41.11673

Yao G, Yin M, Lian J et al (2010) MicroRNA-224 is involved in transforming growth factor-β-mediated mouse granulosa cell proliferation and granulosa cell function by targeting Smad4. Mol Endocrinol 24:540–551. https://doi.org/10.1210/me.2009-0432

Yin M, Wang X, Yao G et al (2014) Transactivation of microRNA-320 by microRNA-383 regulates granulosa cell functions by targeting E2F1 and SF-1 proteins. J Biol Chem 289:18239–18257. https://doi.org/10.1074/jbc.M113.546044

Yuan S, Ortogero N, Wu Q et al (2014) Murine follicular development requires oocyte DICER, but not DROSHA1. Biol Reprod. https://doi.org/10.1095/biolreprod.114.119370

Zhang M, Zhang Q, Hu Y et al (2017a) miR-181a increases FoxO1 acetylation and promotes granulosa cell apoptosis via SIRT1 down-regulation. Cell Death Dis 8:e3088. https://doi.org/10.1038/cddis.2017.467

Zhang Y-L, Wang R-C, Cheng K et al (2017b) Roles of Rap1 signaling in tumor cell migration and invasion. Cancer Biol Med 14:90–99. https://doi.org/10.20892/j.issn.2095-3941.2016.0086